Synergistic effect of ibrutinib and CD19 CAR-T cells on Raji cells in vivo and in vitro

Meijing Liu
Tianjin Medical University
Xuelin Wang
Institute of Developmental Biology and Molecular Medicine, Fudan University, Shanghai, China
Zheng LI
The First Central Clinical College of Tianjin Medical University, Tianjin, China
Rui Zhang
Department of Hematology, Tianjin First Central Hospital, Tianjin, China
Juan Mu
Department of Hematology, Tianjin First Central Hospital, Tianjin, China
Yanyu Jiang
Department of Hematology, Tianjin First Central Hospital, Tianjin, China
Lei Sun (lei_sun@fudan.edu.cn)
Institute of Developmental Biology and Molecular Medicine, Fudan University, Shanghai, China
Qi Deng (kachydeng@126.com)
Department of Hematology, Tianjin First Central Hospital, Tianjin, China https://orcid.org/0000-0002-3646-4953

Research

Keywords: Bruton tyrosine kinase inhibitor, Chimeric antigen receptor, Programmed cell death 1 ligand 1, Raji cell line, Tumor microenvironment

Posted Date: April 15th, 2020

DOI: https://doi.org/10.21203/rs.3.rs-21887/v1

Version of Record: A version of this preprint was published at Cancer Science on September 15th, 2020. See the published version at https://doi.org/10.1111/cas.14638.

Abstract

Background Ibrutinib might improve the efficacy of CD19 CAR-T cell therapy in chronic lymphocytic leukemia (CLL). We expect to study the possibility and mechanism of synergistic effect of ibrutinib and CAR-T cells in other types of lymphoma. Methods We selected the CD19 CAR-T cells of a patient who failed in this therapy and a dose of 8 mg/kg/day ibrutinib to study the synergistic effect. Subcutaneous and tail vein tumorigenic mice were established with Raji cells. The differences of the synergistic effect between these two models were compared by bioluminescence imaging (BLI) monitoring and flow cytometry (FCM). Then the expression of STAT-3 signaling pathway was assessed by western blot analysis. Results The expression of PD-L1 was 0.23±0.06% in Raji cells. In subcutaneous tumorigenic model, the luciferase signal was reduced significantly in the ibrutinib combined with CD19 CAR-T cell group. The proportion of CD19 CAR-T cells was higher in the polytherapy group than that of the CAR-T cell monotherapy group. But we didn't get analogous synergistic effect in tail vein tumorigenic model. There was no difference between the STAT-3 signaling pathway expression in residual tumor cells with or without ibrutinib. Conclusions Our result might indicate that no IL-10/STAT-3/PD-L1 pathway were involved in the synergistic effect. Then some other mechanism about tumor microenvironment might be a possible target for ibrutinib. We expect our results provide evidence for the use of ibrutinib in polytherapy to other types of B cell lymphoma.

Background

As a BTK inhibitor, ibrutinib controls the homing and migration of tumor cells by downregulating NF-κB signaling. It is important to block the interactions between macrophages and tumor cells[1–4]. Abnormal B-cell receptor (BCR) signaling is a key mechanism of B-cell malignancy disease progression. BTK has a pivotal role in BCR signaling [5, 6]. By blocking the BTK, ibrutinib is able to inhibit BCR signaling in cells of B-cell malignancies[7, 8]. It has been approved by FDA for the treatment of chronic lymphocytic leukemia (CLL) [9] and mantle cell lymphoma (MCL)[10] in all lines of therapy. Moreover, ibrutinib has been used widely in different types of B malignancies of the lymphatic system[11–13]. Although the overall response rates (ORR) to ibrutinib in CLL or MCL patients is high, the complete response (CR) rate is low, and some patients experience disease progression while receiving ibrutinib[14, 15].

CAR-T cell therapy achieved high response rates in patients with relapsed/refractory (R/R) diffuse large B-Cell lymphoma (DLBCL)[16, 17] and R/R B acute lymphoblastic leukemia (B-ALL)[18]. Additionally, CD19 CAR-T cell therapy was also used in CLL [19, 20], but the efficacy was lower for CLL than DLBCL and B-ALL [16–18]. A study evaluating safety and feasibility of CD19 CAR-T cell therapy in CLL patients who received ibrutinib suggested that ibrutinib might improve the efficacy of CD19 CAR-T cell therapy[21]. A similar synergistic effect was reported in MCL models[22]. With the assistance of ibrutinib, the cytotoxicity of CD19 CAR-T cells to MCL cells was significantly enhanced. In our study, Raji cell line was selected for polytherapy study of ibrutinib and CD19 CAR-T cell in vitro and in vivo. A synergistic effect of ibrutinib combined with CD19 CAR-T cell was observed in subcutaneous tumorigenic model but not the

tail vein tumorigenic model, together these data suggest that some other mechanism about tumor microenvironment might be a possible target for ibrutinib.

Material And Methods

Primary cells and cell lines

Nine R/R DLBCL patients were enrolled in a clinical trial at the Department of Hematology in Tianjin First Center Hospital (Tianjin, China) and received CD19 CAR-T cell expressing anti-CD19 scFv and 4-1BB-CD3ζ costimulatory-activation domains therapy (*ChiCTR1800018059*). All the patients or their representatives provided informed consent before enrollment. They agreed with the use of his specimens and data for our study.

Raji and EHEB cells (American Type Culture Collection, ATCC, Manassas, VA, USA) were cultured in RPMI-1640 medium (Gibco; Thermo Fisher Scientific, Inc. Waltham, MA, USA) containing 10% fetal bovine serum (FBS) (Gibco, Thermo Fisher Scientific, Inc.) and 50 UI/ml penicillin/streptomycin (Gibco, Life Technologies). The human embryonic kidney 293 (Lenti-X-293T) cells (ATCC) were maintained in Dulbecco's Modified Eagle Medium (DMEM) (Sigma-Aldrich, USA), supplemented with 10% FBS and 50 UI/mL penicillin/streptomycin.

Isolation of peripheral blood mononuclear cells (PBMCs) and transduction of T cells.

PBMCs were isolated by Ficoll density gradient centrifugation. $CD3^+$ T cells were selected by MACS using CD3 microbeads (Miltenyi Biotec, Inc, Cambridge, MA, USA) from the PBMCs. $CD3^+$ T cells were stimulated by anti-CD3/anti-CD28 mAb-coated Human T-Expander beads (Cat. no. 11141D; Thermo Fisher Scientific, Inc. Waltham, MA, USA) and cultured in T-cell medium X-Vivo 15 (Lonza Group, Ltd., Basel, Switzerland) supplemented with 250 IU/mL interleukin-2 (IL-2; Proluekin; Novartis International AG, Basel, Switzerland). On the fourth day of cultivation, T cells ($3x10^6$) were transduced with a lentiviral vector encoding anti-CD19 CAR constructs (5 μg; lenti-EF1a-CD19-2rd-CAR; Creative Biolabs, Inc., Shirley, NY, USA) and cultured in media containing recombinant human IL-2 (30 U/ml). At the same time, CD3+ T cells were cultured in T-cell medium X-Vivo 15 supplemented with 250 IU/mL interleukin-2. On the 12th day of cultivation, the transduction efficiency of CD19 CAR -T cells were analyzed by flow cytometry (FCM).

Pharmacologic agents

The BTK inhibitor Ibrutinib was provided by Xian Janssen pharmaceutical co. Ltd. Ibrutinib was dissolved in Dimethyl sulfoxide (DMSO) to make a 20 μM stock solution and stored in small aliquots at −20°C.

The proliferation of CD19 CAR-T cells and cell lines in vitro

The effects of different doses of ibrutinib on CD19 CAR-T cells or cell lines proliferation were determined by Cell Counting Kit-8 (CCK-8; Dojindo Molecular Technologies, Inc. Kumamoto, Japan). CD19 CAR-T cells

or cell lines were seeded in 96-well plates with $3x10^4$ cells per well and treated with various doses of single-agent ibrutinib. The absorbances were measured at 450 nm at 24h, 48h and 72h with an enzyme standard instrument. All assays were run in duplicates or triplicates.

The expression of programmed cell death protein 1 (PD-1) on CAR-T cells, programmed cell death 1 ligand 1 (PD-L1) on cell lines and immune phenotype of T lymphocyte

In the preparation process of CD19 CAR-T cells, the expression of PD-1 was analyzed by FCM. When the CAR-T cells were harvested, the expression of PD-1 was analyzed by FCM in the co-culture system containing ibrutinib or Raji cells at 24h and 48h. The effective target ratio was 1:1 and the concentration of ibrutinib is 5 μM. The expression of PD-L1 in Raji and EHEB cells were analyzed by FCM.

The T lymphocyte immune phenotype of the nine patients were detected after the T lymphocytes were cultured with 5 μM of ibrutinib for 72h in vitro. The analysis included the naive T cells, effector T cells, central memory T cells and effector memory T cells in $CD3^+CD4^-CD8^+$ T cells and $CD3^+CD4^+CD8^-$ T cells. We evaluated the percentage and absolute numbers of T cells of various subsets.

Cytotoxicity and the interferon-γ (IFN-γ) assays

The cytotoxicity assay was carried out with the effective target ratio of 1:1 for 24h and 48h in the absence of supplemented cytokines. The concentration of ibrutinib was at 0μM, 1μM and 10 μM combined with CD19 CAR-T cells respectively. As controls, targets ($2x10^4$ cells per well) and effectors ($2x10^4$ cells per well) combined with 0μM, 1μM and 10 μM ibrutinib respectively were simultaneously incubated to determine spontaneous cell death and cell death caused by drug toxicity. Cytotoxicity was detected by lactate dehydrogenase (LDH) cytotoxicity test kit (Dojindo Molecular Technologies, Inc.) at 490 nm. Collected the supernatant after cell lines cultured with CD19 CAR-T cells of nine R/R DLBCL patients for 48h respectively. The release of IFN-γ was detected using an ELISA kit (BD Biosciences) according to the manufacturer's directions. All assays were run in duplicates or triplicates.

Xenograft Tumor Model

Six-week old female CAnN.Cg-Foxn1nu/CrlVR (BALB/c) mice weighing 20.12±1.45 g (n=50; Beijing Vitonlihua Experimental Animal Technology Co., Ltd, Beijing, China) received $1x10^7$ Raji cells transduced with luciferase (purchased from Shanghai Suer Biotechnology Co.) by subcutaneous injection, followed by bioluminescence imaging (BLI) monitoring twice a week. Upon confirmation of engraftment after 25 days, the mice were randomized into ibrutinib (8 mg/kg/day) monotherapy group, CD19 CAR-T cell ($2x10^7$/kg) monotherapy group, ibrutinib combined with CD19 CAR-T cell group and ibrutinib combined with T cell ($2x10^7$/kg) group. The CD19 CAR-T cells and T cells generated from the same donor (The patient 7# who did no response to CAR-T cell therapy) were administered by tail vein on day 0. Ibrutinib was administered daily by oral gavage to the mice. There were five mice in each group. On 0, 14 and 28 day, mice were monitored with bioluminescent imaging for disease progression following intraperitoneal injection with D-luciferin (Goldbio,150 mg/kg) 10 min before scanning. Before imaging, mice were

anesthetized via a nose cone with 2% isoflurane (Zoetis, UK)/medical oxygen and maintained under inhalational anesthesia. All mice were sacrificed when either experimental or humane endpoints were reached.

Another group of the same mice were injected with $1x10^7$ Raji lymphoma cells through tail vein (iv) injection to establish animal models. Upon confirmation of engraftment after 10 days, these mouse models were separated randomly into various groups as the subcutaneous tumorigenic mouse models. The CD19 CAR-T cells, T cells and ibrutinib were utilized in the same way as subcutaneous tumorigenic mouse models also. There were five mice in each group. The proportions of lymphoma cells in epicanthus vein were analyzed by FCM.

Change of CD19 CAR-T cells ratio in mice

Inner canthus blood was collected from the mice of CAR T-cell group and ibrutinib combined with CAR-T cell group on 0, 7,14, 21 and 28 day. The proportions of CD19 CAR-T cells in mice were analyzed by FCM.

Western blot analysis of phos-signal transducer and activator of transcription 3 (STAT-3)

In subcutaneous tumorigenic model, we chose the ibrutinib group and the CD19 CAR-T cells and ibrutinib polytherapy group in the following western blot analysis. The residual tumor tissue in subcutaneous nodules were taken and milled to obtain tumor cells after the mice were sacrificed after 28 days of therapy. Then tumor cells were selected by CD19 magnetic beads for the following experiments. CD19 positive tumor cells (Raji cells) were plated at $0.5x10^6$ per well (6 well plate) for 0h, 24h and 72h. Cells were collected and dissolved in 200uL laemmli buffer (Bio-Rad, Hercules, CA, USA). 10μL of each protein sample was loaded on SDS-Page gel (Bio-Rad) and transferred to PVDF membrane. Antibodies of STAT-3 (Ser727), STAT-3 and GAPDH were applied and detected by corresponding secondary antibodies. The total and phosphorylated proteins were detected using the enhanced chemiluminescence detection system.

Statistical analysis

All statistical analyses were performed using GraphPad Prism 7 (GraphPad Software, Inc., La Jolla, CA, USA) and SPSS version 23 (IBM Corp. Armonk, NY, USA). Data are expressed as the mean ± Standard Deviationor (SD) or standard errors of the mean (SEM), *t* test were used where indicated. Then analysis of variance (Student-newman-Keuls method) was used for pantwise comparison. Differences were considered significant at values of $P<0.05$.

Results

Patient characteristics

Five male and four female R/R DLBCL patients with a median age of 49.9 (range: 25-68) years old were enrolled in a clinical trial. The molecular subtypes, the stages according to the modified Ann Arbor

staging system and the international prognostic index (IPI) scores were shown in Table 1.

Transduction efficiency of CD19 CAR-T cells

The titer of anti-CD19-CAR virus was $3x10^8$ TU/ml. The mean anti-CD19-CAR transduction efficiency of the nine relapse/refractory DLBCL patients was 58.49±6.50%.

The effect of different doses of single-agent ibrutinib on the proliferation of CD19 CAR-T cells and different cell lines

To analyze how ibrutinib and CAR-T cells work together, the influence of ibrutinib on proliferation of CAR-T cells was investigated first. On the 12th day of cultivation, the CD19 CAR-T cells were incubated with ibrutinib at dose of 1μM, 10μM and 20 μM. We determined the inhibition of ibrutinib on CD19 CAR-T cells. Cell growth inhibition as measured by cell density was detectable following 24h, 48h and 72h (Fig. 1a). Noticeably higher ibrutinib concentration meant less survival of CAR-T cells. 72h treatment with 10μM and 20 μM ibrutinib almost swept out the CAR-T cells incubation, which indicates the importance of a proper ibrutinib dosage in the polytherapy strategy. One thing should be pointed out that this experiment setting was target cell free.

We next analyzed the toxicity of ibrutinib on B malignant cells in vitro. Cell survival was measured in EHEB cells and Raji cells treated with ibrutinib at 1μM, 10μM and 20 μM doses for 24h and 48h. The proliferation inhibitions of 20 μM ibrutinib group to EHEB cells and Raji cells at 48h were higher than that of 1μM and 10 μM ibrutinib groups (Fig. 1b-c).

The cytotoxicity of CD19 CAR-T cells to EHEB cells or Raji cells

The CD19 CAR-T cell monotherapy was conducted to test the cytotoxicity capability of CAR-T cells from different patients in vitro. CD19 CAR-T cells were co-cultured with Raji cells or EHEB cells to determine the cytotoxicity using the LDH assay. It showed significant cytotoxicity of CD19 CAR T-cells of patient 1# to 6#, 8# and 9# to EHEB cells or Raji cells (The effective target ratio was 1:1) at 24 and 48h. But the CD19 CAR-T cells of patient 7# showed limited cytotoxicity to EHEB cells or Raji cells at 24 and 48h (Fig. 1d-e). It showed significant release of IFN-γ in CD19 CAR T-cells of patient 1# to 6#, 8# and 9# cultivated with EHEB cells or Raji cells at 48h. But it showed limited release of IFN-γ to EHEB cells or Raji cells in patient 7# (Fig. 1f).

The combined effect of ibrutinib and CD19 CAR-T cells

The cytotoxicity of CD19 CAR-T cells combined with ibrutinib at 0μM, 1μM and 10 μM doses at 24h and 48h after co-culture with EHEB cells and Raji cells was analyzed. It showed no combined effects of CD19 CAR-T cells (patient 1# to 6#, 8# and 9#) with ibrutinib to EHEB cells or Raji cells (The effective target ratio was 1:1) at 24 and 48h. The CD19 CAR-T cells of patient 7# showed almost no cytotoxicity to EHEB cells or Raji cells with ibrutinib at 24h and 48h (Fig. 2a-b). In the clinical, CD19 CAR-T cell treatment failed

in patient 7#. The neck neoplasm of this patient increased further 14 days after CD19 CAR-T cell treatment (Fig. 2c).

The changes of PD-1 expression in CAR-T cells co-cultured with ibrutinib and Raji cells, the PD-L1 expression in cell lines

The mean expression of PD-1 in T cells of the nine patients before CAR-T cell preparation was 62.40±8.46%. When the CAR-T cells were harvested at day 14, the PD-1 expression in CAR-T cells declined to 2.33±0.69% in vitro (Fig. 2d). But the harvested CD19 CAR-T cells were co-cultured with ibrutinib and Raji cells, the PD-1 expressions increased in CAR-T cells co-cultured with Raji cells after 48h. While the PD-1 expressions in CAR-T cells co-cultured with ibrutinib and Raji cells were lower than that of co-cultured with Raji cells only (Fig. 2e). Three repetitions of the experiment resulted in that the expression of PD-L1 was 0.23±0.06% in Raji cells and 32.83±3.18% in EHEB cells.

The immune phenotype of T lymphocyte in all the nine patients

We evaluated the various subset percentage and absolute numbers of T cells cultured with 5 μM of ibrutinib in the nine patients. There was no difference between the percentage and absolute numbers of the naive T cells, effector T cells, central memory T cells and effector memory T cells in $CD3^+CD4^-CD8^+$ T cells and $CD3^+CD4^+CD8^-$ T cells (Fig. 3).

Antitumor efficacy of ibrutinib and CD19 CAR-T cells in subcutaneous tumorigenic model

We performed the following mouse experiments with the CD19 CAR-T cells of the patient 7# who had failed in CD19 CAR-T cell therapy. In the subcutaneous tumorigenic model, the single agent ibrutinib, CD19 CAR-T cell, ibrutinib combined with CD19 CAR-T cell, and ibrutinib combined with T cell group mice presented no detectable toxicities and maintained overall weight. The CD19 CAR-T cell alone exhibited limited efficacy and could not even weaken the tumor size. In contrast, the reduction in tumor size was greater in the polytherapy group than those in the ibrutinib group (P_{day28}=0.0003) and the ibrutinib combined with T cell group (P_{day28}=0.0027). (Fig. 4a, c). The extinction in luciferase expression was greater in the polytherapy group than those in the other three groups (Fig. 4b). More importantly, the polytherapy group had a best efficacy indicating an additive effect between ibrutinib and CD19 CAR-T cell.

In subcutaneous tumorigenic model, the proportions of CD19 CAR-T cells in the CD19 CAR-T cell monotherapy group and the CD19 CAR-T cells and ibrutinib polytherapy group were analyzed. There was no difference of the proportion of CD19 CAR-T cells in the two groups on day 7 and day 14 (P_{day7}=0.1394, P_{day14}=0.0812). The proportion of CD19 CAR-T cells then began to increase and almost double on day 21 in the polytherapy group, a proven sign of robust CAR-T cell activation and consequent cytotoxicity, which was absent in the monotherapy group. (P_{day21}=0.0015, P_{day28}=0.0207) (Fig. 4d).

Antitumor efficacy of ibrutinib and CD19 CAR-T cells in tail vein tumorigenic model

In the tail vein tumorigenic model, the proportion of lymphoma cells in the CD19 CAR-T cell monotherapy group increased quickly, causing the mice to die quickly after 21 days of treatment. There was no difference of the proportion of lymphoma cells in the polytherapy group, the ibrutinib monotherapy group and the ibrutinib combined with T cell group (F_{day14}=0.6925, F_{day21}=0.9951, F_{day28}=1.1136) (P_{day14}=1.0067, P_{day21}=0.6609, F_{day28}=0.4502) (Fig. 5a).

In the tail vein tumorigenic model, the proportion of CD19 CAR-T cells first increased at day 7, which meant the activation of CAR-T cells, and then declined quickly, probably due to the tumor cell proliferation overwhelming the blood stream. It was known that tail vein model was favored by Raji cells as it could progress quickly (Fig. 5b).

Western blot analysis of STAT-3 expression

In the subcutaneous tumorigenic model, the effect was greater in the polytherapy group than that of in the ibrutinib monotherapy group. We obtained residual tumor cells from these two groups of mouse model. Then we analyzed the effects of ibrutinib with or without CD19 CAR-T cells on the expression of STAT-3 signaling pathway in Raji cells. The results demonstrated that there was no difference between the expression of STAT-3 in groups of ibrutinib combined with or without anti-CD19 CAR T-cells (Fig. 6).

Discussion

Experiences in the use of CD19 CAR-T cells to treat R/R CLL are limited. Recently, a review described the published results about the CD19 CAR-T cell therapy to CLL since the first efficacy report of this therapy in 2011[19, 23]. The efficacy CR was obtained only in 20-30% of R/R CLL patients [23], and progression-free survival (PFS) estimated at about 25% at 18 months [21, 22, 24]. It was lower for CLL than for B-ALL and DLBCL[16-19]. The main reason might be related to T cell dysfunction in CLL patients, resulting in the decreased amplification and activity of CD19 CAR-T cells [25-27].

As an orally BTK inhibitor, ibrutinib is capable to motivate redistribution of B malignant cells into peripheral blood, which eventually leads to obvious shrink of enlarged lymph nodes[28, 29]. Therefore, ibrutinib has high ORR and long-lasting remission in patients with CLL or MCL. Ibrutinib treatment to CLL patients for more than five months could improve the proliferation and cytotoxic activity of T cells and their CD19 CAR-T cells[26]. Meanwhile, expression level of immunosuppressive marker programmed death-1 (PD-1) was detected to be decreased, which might explain the function restoration of these T cells after prolonged ibrutinib treatment. Moreover, such clinical curative effects of CD19 CAR-T cell therapy could be reproduced in those patients experiencing failure of ibrutinib therapy[21]. It will be of value to explore whether ibrutinib has the homologous beneficial effect in other B malignance.

In addition to CLL, a similar synergistic effect between ibrutinib and CD19 CAR-T cell was reported for MCL cell line[22]. However, its working concentrations of ibrutinib were 25 mg/kg/day and 125 mg/kg/day, which is overly above the clinically recommended dose of ibrutinib. Because of the concern that excessive doses of ibrutinib might inhibit CAR-T cells proliferation, in this study we chose the

clinically recommended dose ibrutinib (8 mg/kg/day). Meanwhile, we selected a case of inept CD19 CAR-T cell to investigate the synergistic effect of CAR-T cells with ibrutinib on Raji cell line in vitro and in vivo. No synergistic effect was observed in vitro and in the tail vein tumorigenic mouse model. Interestingly, we confirmed the ibrutinib combined with CD19 CAR-T cell synergistic effect in subcutaneous tumorigenic mice. What is the reason for the different results of the two tumorigenesis methods in mice? It is possible that the complex tumor microenvironment in subcutaneous tumorigenic mouse model contribute to this synergistic effect. Further studies would need to confirm this mechanism.

The mechanisms by which ibrutinib enhances T cell function is still not very clear. Ibrutinib could enhance the function of CLL patient T cells through BTK-dependent and BTK-independent mechanisms[27]. A study showed that ibrutinib modulated the tumor microenvironment and reduced the immune-suppressive by downregulating the expression of programmed death ligand-1 (PD-L1) on CLL cells[30]. Their further analysis showed that this effect was mediated through inhibition of the STAT3 pathway in CLL cells[30]. A related study found that BTK inhibitors blocks both NFATc1 and STAT3 activation, thereby inhibiting IL-10 and PD-L1 expression[31]. Another study showed that ibrutinib markedly increased $CD4^+$ and $CD8^+$ T cell numbers and reduced the PD-1 and CTLA-4 expression in CLL patients. It might be due to diminished activation-induced cell death through IL-2-inducible T cell kinase (ITK) inhibition[27]. Inhibition of ITK activity leads to the inhibition of Th2 cell differentiation and the promotion of Th1 cell immune response[31]. It might be involved in the T cells in CLL patients from Th2 cells to Th1 cells. Further, in CD19 CAR-T cell therapy, ibrutinib may promote the expansion, maintenance, and cytotoxicity of CD19 CAR-T cells in vitro[27, 31, 32]. All the findings revealed PD-L1 expression could be modulated by small molecule inhibitors to potentiate immunotherapies. In our study, the synergistic effect was greater in the ibrutinib combined with CD19 CAR-T cell group than that of in ibrutinib group in Raji cell subcutaneous tumorigenic mouse model rather than in tail vein tumorigenic model. But there was no difference between the expression of STAT-3 in groups of ibrutinib with or without CD19 CAR-T cells. Meanwhile, the expression of PD-L1 was only 0.23±0.06% in Raji cells. This result might indicate that non-IL-10/STAT-3/PD-L1 pathways were involved in the synergistic effect. It suggested that some other mechanism about tumor microenvironment might be a possible target for ibrutinib.

In our study, we chose the CD19 CAR-T cells generated from patient 7# who did no response to CAR-T cell therapy, and the Raji cell which does not express PD-L1. The Raji cell subcutaneous tumorigenic mouse model received the clinically recommended dose ibrutinib for only 28 days. We did not obtain the results that ibrutinib and CD19 CAR-T cells had a synergistic effect on Raji cells in vitro. It was not as same as the results of studies before on MCL cell line[27, 31, 32]. But ibrutinib could improve the curative effect of CD19 CAR-T cells in Raji cell subcutaneous tumorigenic mice. Does our results suggest that tumor microenvironment might be a possible target for ibrutinib, rather than by the STAT-3 signaling pathway? Further studies would be required for the mechanisms and to provide evidence for the use of ibrutinib in polytherapy with other types of B cell lymphoma.

Conclusions

The synergistic effect of ibrutinib and CD19 CAR-T was greater than ibrutinib or CD19 CAR-T monotherapy in Raji cell subcutaneous tumorigenic mouse model rather than in tail vein tumorigenic model. We further discussed that the mechanisms of synergistic effect might be related with the tumor microenvironment rather than STAT-3 signaling pathway.

Abbreviations

CD19 CAR: anti-CD19 chimeric antigen receptor

Declarations

Ethics approval and consent to participate This study was approved by the Medical Ethics Committee of the Department of Hematology, Tianjin First Center Hospital (Tianjin, China). (Approved No. of ethic committee: 2018N105KY). The patient gave their written informed consent in accordance with the Declaration of Helsinki. This Clinical trial is registered at http://www.chictr.org.cn/index.aspx as *ChiCTR1800018059*. The patient agreed to the use of his specimens and data for our study. All animal procedures were approved by the institutional animal and care use committee of Tianjin First Central Hospital (Tianjin, China).

Consent for publication All subjects have written informed consent.

Availability of data and materials The datasets used and/or analyzed during the current study are available from the corresponding author on reasonable request.

Competing interests The authors declare that they have no competing interests

Funding Not applicable

Authors' contributions In this study, QD contributed to concept and design; MJL, XLW contributed to experiment performance and data collection; MJL and LS contributed to manuscript preparation; MJL, JM, YYJ and ZL contributed to analysis and interpretation of data; All these works were supervised by QD and LS; All authors read and approved the final manuscript.

Acknowledgements: We thank the patients for their participation in our experimental studies and clinical trials.

References

1. Saleh LM, et al. Ibrutinib downregulates a subset of miRNA leading to upregulation of tumor suppressors and inhibition of cell proliferation in chronic lymphocytic leukemia. Leukemia. 2017;31(2):340-349.
2. Chang BY, et al. Egress of CD19(+)CD5(+) cells into peripheral blood following treatment with the Bruton tyrosine kinase inhibitor ibrutinib in mantle cell lymphoma patients. Blood.

2013;122(14):2412-2424.
3. Cheng S, et al. BTK inhibition targets in vivo CLL proliferation through its effects on B-cell receptor signaling activity. Leukemia. 2014;28(3):649-657.
4. Ponader S, et al. The Bruton tyrosine kinase inhibitor PCI-32765 thwarts chronic lymphocytic leukemia cell survival and tissue homing in vitro and in vivo. Blood. 2012;119(5):1182-1189.
5. DK. M, BF. N, Hussain A, MO. u, AJ. M, CI. S. Dual Phosphorylation of Btk by Akt/Protein Kinase B Provides Docking for 14-3-3□, Regulates Shuttling, and Attenuates both Tonic and Induced Signaling in B Cells. Molecular and cellular biology. 2013;33(16):3214-3226.
6. Ponader S, Burger JA. Bruton's tyrosine kinase: from X-linked agammaglobulinemia toward targeted therapy for B-cell malignancies. J Clin Oncol. 2014;32(17):1830-1839.
7. Advani RH, et al. Bruton tyrosine kinase inhibitor ibrutinib (PCI-32765) has significant activity in patients with relapsed/refractory B-cell malignancies. J Clin Oncol. 2013;31(1):88-94.
8. Herman SEM, et al. Ibrutinib inhibits BCR and NF-κB signaling and reduces tumor proliferation in tissue-resident cells of patients with CLL. Blood. 2014;123(21):3286-3295.
9. Byrd JC, et al. Targeting BTK with ibrutinib in relapsed chronic lymphocytic leukemia. The New England journal of medicine. 2013;369(1):32-42.
10. Wang ML, et al. Targeting BTK with ibrutinib in relapsed or refractory mantle-cell lymphoma. The New England journal of medicine. 2013;369(6):507-516.
11. Rule S, et al. Ibrutinib versus temsirolimus: 3-year follow-up of patients with previously treated mantle cell lymphoma from the phase 3, international, randomized, open-label RAY study. Leukemia. 2018;32(8):1799-1803.
12. Buggy JJ, Elias L. Bruton Tyrosine Kinase (BTK) and Its Role in B-cell Malignancy. International Reviews of Immunology. 2012;31(2):119-132.
13. Schliffke S, et al. Clinical response to ibrutinib is accompanied by normalization of the T-cell environment in CLL-related autoimmune cytopenia. Leukemia. 2016;30(11):2232-2234.
14. Jain P, et al. Outcomes of patients with chronic lymphocytic leukemia after discontinuing ibrutinib. Blood. 2015;125(13):2062-2067.
15. Maddocks KJ, et al. Etiology of Ibrutinib Therapy Discontinuation and Outcomes in Patients With Chronic Lymphocytic Leukemia. JAMA Oncology. 2015;1(1):80.
16. Neelapu SS, et al. Axicabtagene Ciloleucel CAR T-Cell Therapy in Refractory Large B-Cell Lymphoma. The New England journal of medicine. 2017;377(26):2531-2544.
17. Schuster SJ, et al. Tisagenlecleucel in Adult Relapsed or Refractory Diffuse Large B-Cell Lymphoma. The New England journal of medicine. 2019;380(1):45-56.
18. Maude SL, et al. Tisagenlecleucel in Children and Young Adults with B-Cell Lymphoblastic Leukemia. The New England journal of medicine. 2018;378(5):439-448.
19. Porter DL, Levine BL, Kalos M, Bagg A, June CH. Chimeric antigen receptor-modified T cells in chronic lymphoid leukemia. The New England journal of medicine. 2011;365(8):725-733.

20. Porter. DL, et al. Chimeric antigen receptor T cells persist and induce sustained remissions in relapsed refractory chronic lymphocytic leukemia. Science translational medicine. 2015;7(303):303ra139.
21. CJ. T, et al. Durable Molecular Remissions in Chronic Lymphocytic Leukemia Treated With CD19-Specific Chimeric Antigen Receptor-Modified T Cells After Failure of Ibrutinib. J Clin Oncol. 2017;35(26):3010-3020.
22. Ruella M, et al. The Addition of the BTK Inhibitor Ibrutinib to Anti-CD19 Chimeric Antigen Receptor T Cells (CART19) Improves Responses against Mantle Cell Lymphoma. Clinical cancer research : an official journal of the American Association for Cancer Research. 2016 22(11):2684-2696.
23. Lemal R, Tournilhac O. State-of-the-art for CAR T-cell therapy for chronic lymphocytic leukemia in 2019. Journal for immunotherapy of cancer. 2019;7(1):202.
24. Fraietta JA, et al. Determinants of response and resistance to CD19 chimeric antigen receptor (CAR) T cell therapy of chronic lymphocytic leukemia. Nat Med. 2018;24(5):563-571.
25. Mueller KT, et al. Cellular kinetics of CTL019 in relapsed/refractory B-cell acute lymphoblastic leukemia and chronic lymphocytic leukemia. Blood. 2017;130(21):2317-2325.
26. Fraietta JA, et al. Ibrutinib enhances chimeric antigen receptor T-cell engraftment and efficacy in leukemia. Blood. 2016;127(9):1117-1127.
27. Long M, et al. Ibrutinib treatment improves T cell number and function in CLL patients. The Journal of clinical investigation. 2017 127(8):3052-3064.
28. Burger JA, Montserrat E. Coming full circle: 70 years of chronic lymphocytic leukemia cell redistribution, from glucocorticoids to inhibitors of B-cell receptor signaling. Blood. 2013;121(9):1501-1509.
29. Burger JA, et al. Safety and activity of ibrutinib plus rituximab for patients with high-risk chronic lymphocytic leukaemia: a single-arm, phase 2 study. The Lancet Oncology. 2014;15(10):1090-1099.
30. Kondo K, et al. Ibrutinib modulates the immunosuppressive CLL microenvironment through STAT3-mediated suppression of regulatory B-cell function and inhibition of the PD-1/PD-L1 pathway. Leukemia. 2018;32(4):960-970.
31. Dubovsky JA, et al. Ibrutinib is an irreversible molecular inhibitor of ITK driving a Th1-selective pressure in T lymphocytes. Blood. 2013;122(15):2539-2549.
32. Yin Q, et al. Ibrutinib Therapy Increases T Cell Repertoire Diversity in Patients with Chronic Lymphocytic Leukemia. Journal of immunology (Baltimore, Md : 1950). 2017;198(4):1740-1747.

Tables

Table1. Baseline Characteristics of nine patients

Patient number	Age	Sex	Molecular subtype	stage	Previous response status	IPI at enrollment	Primary lines of therapy	Transduction efficiency (%)
P1#	31	female	Non-GCB	III	refractory	3	12	56.3%
P2#	56	male	Non-GCB	IV	relapse	3	8	54.8%
P3#	35	male	Non-GCB	III	relapse	3	8	68.7%
P4#	52	male	Non-GCB	IV	relapse	3	14	66.9%
P5#	54	female	Non-GCB	IV	refractory	3	10	55.1%
P6#	50	male	Non-GCB	IV	relapse	2	12	58.3%
P7#	58	male	Non-GCB	IV	refractory	3	7	61.7%
P8#	63	female	Non-GCB	IV	refractory	5	13	46.5%
P9#	50	female	Non-GCB	IV	refractory	3	20	58.1%

Figures

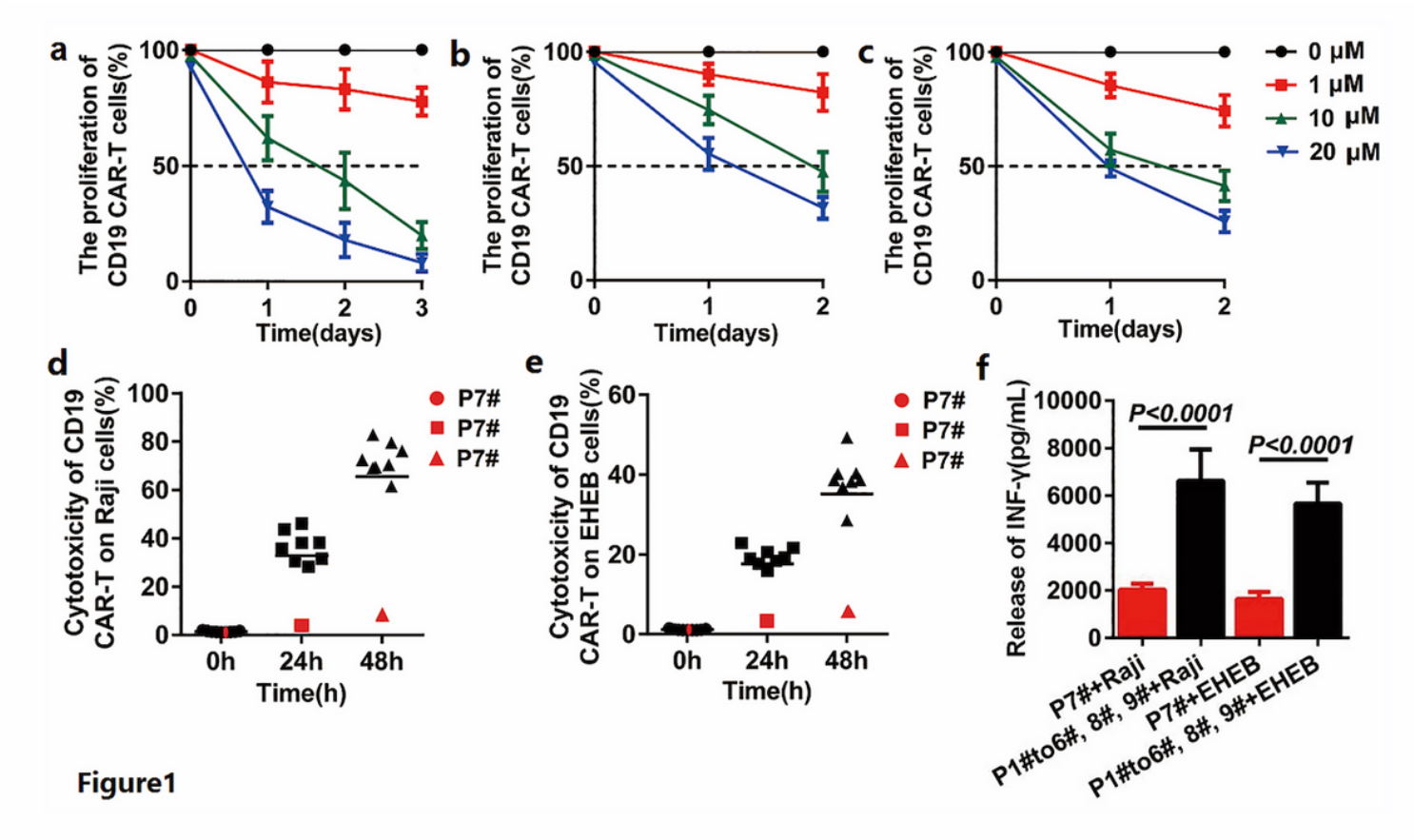

Figure 2

The effect of different doses of ibrutinib on cells. a. The effect of different doses of ibrutinib on CD19 CAR-T cells. b-c. The effect of different doses of ibrutinib on EHEB cells and Raji cells. d. The cytotoxicity

of CD19 CAR-T cells from nine patients to EHEB cells. e. The cytotoxicity of CD19 CAR-T cells from nine patients to Raji cells. f. The releases of IFN-γ in CD19 CAR T-cells of patient 1# to 6#, 8# and 9# cultivated with EHEB cells or Raji cells were obvious at 48h. It showed limited release of IFN-γ to EHEB cells or Raji cells in patient 7#.

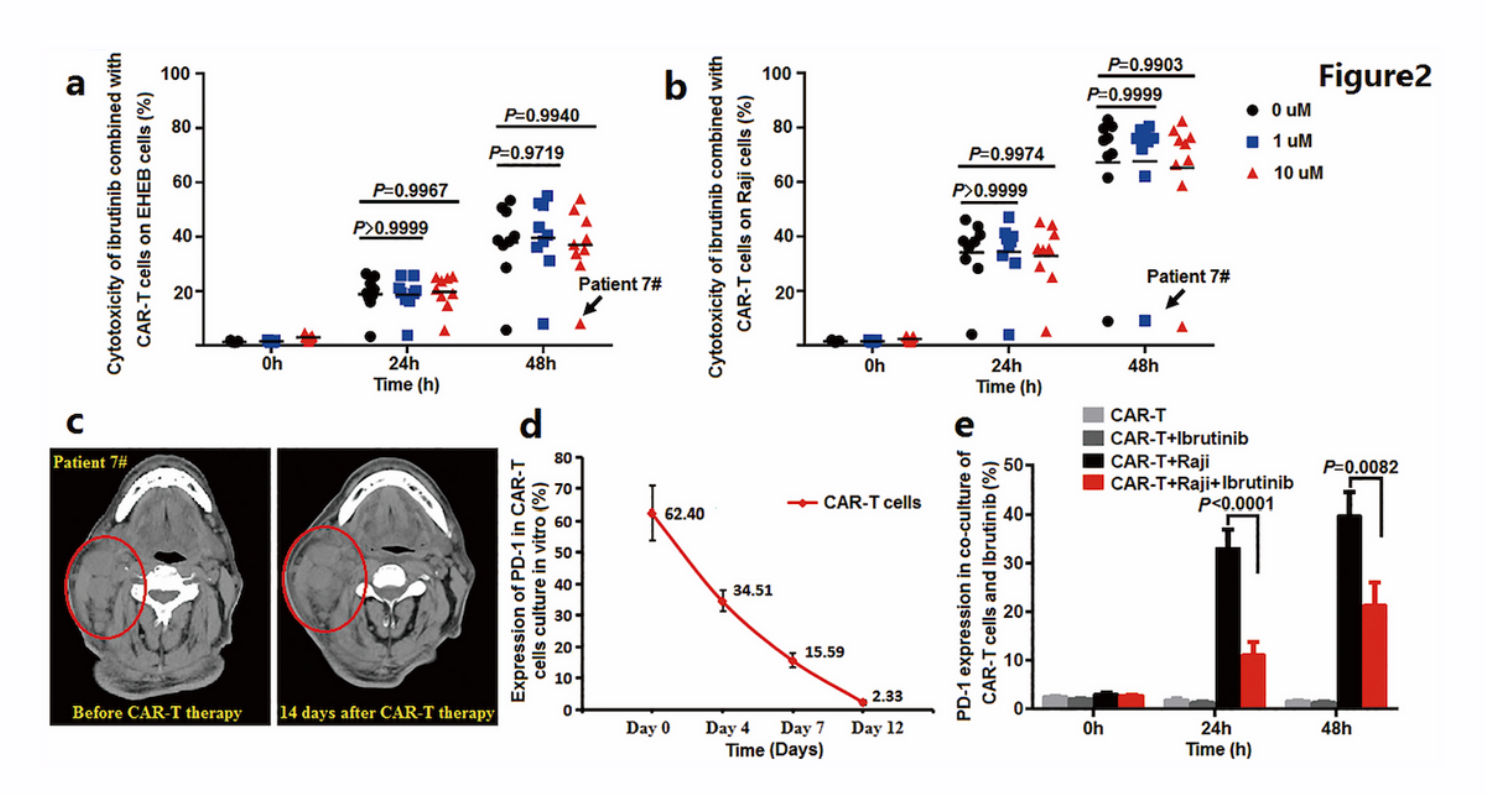

Figure 3

The combined effect of ibrutinib and CD19 CAR-T cells in vitro. a-b. There were no combined effects of CD19 CAR-T cells with ibrutinib on EHEB cells or Raji cells. The CD19 CAR-T cells of patient 7# showed almost no cytotoxicity to cell lines with or without ibrutinib. c. Evaluation of CD19 CAR-T cell therapy effects by computerized tomography in patient 7#. d. The expression of PD-1 in CAR-T cells decreased gradually during the CAR-T cell culture in vitro. e. The expression of PD-1 in CAR-T cells was increased by co-cultured with Raji cells, while it was decreased by co-cultured with ibrutinib and Raji cells. The PD-1 expressions in CAR-T cells co-cultured with ibrutinib and Raji cells were lower than that of co-cultured with Raji cells only.

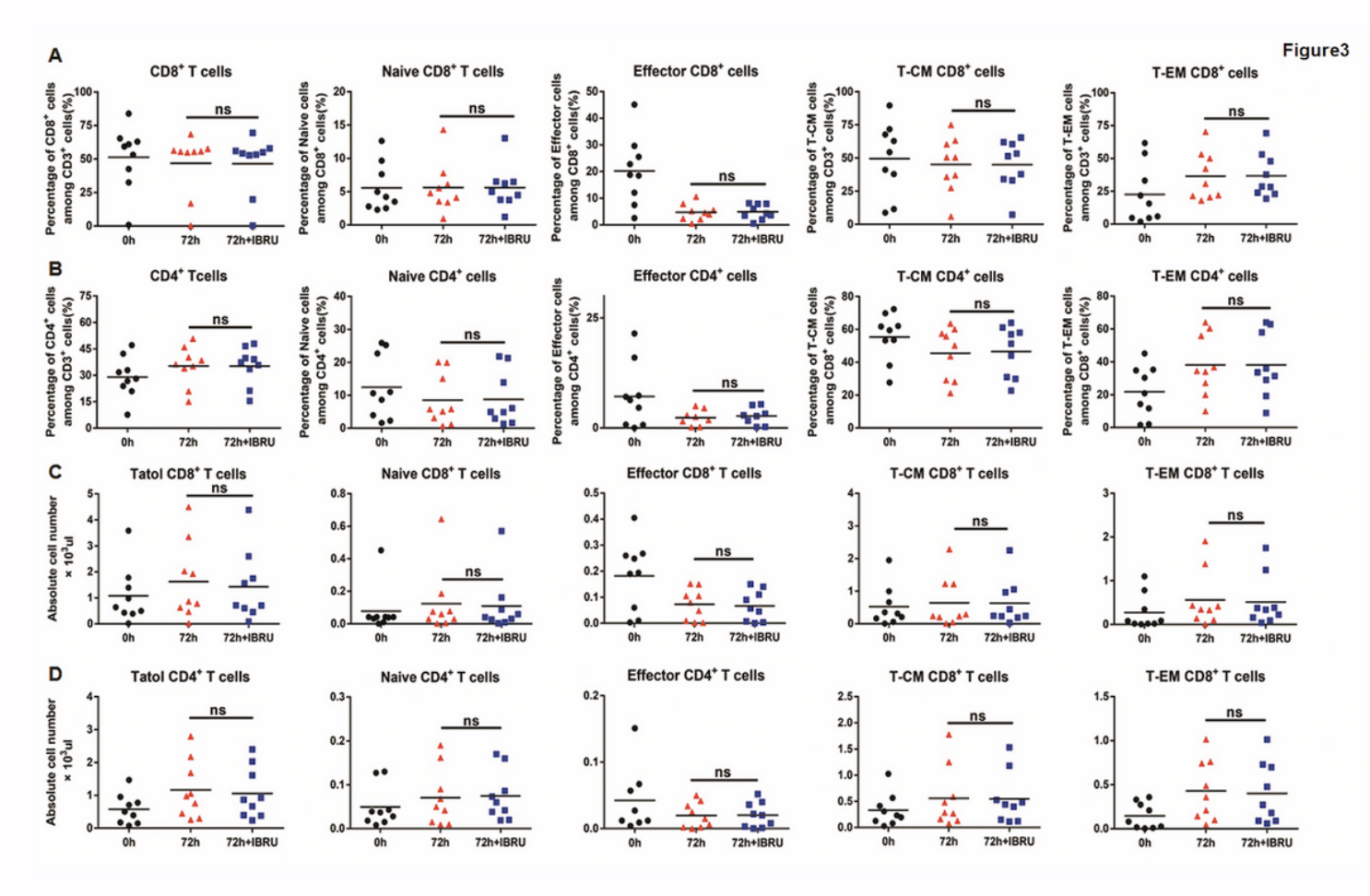

Figure 5

The immune phenotype of T lymphocyte in all the nine patients. There was no difference between the percentage and absolute numbers of the naive T cells, effector T cells, central memory T cells and effector memory T cells in CD3+CD4-CD8+ T cells and CD3+CD4+CD8- T cells.

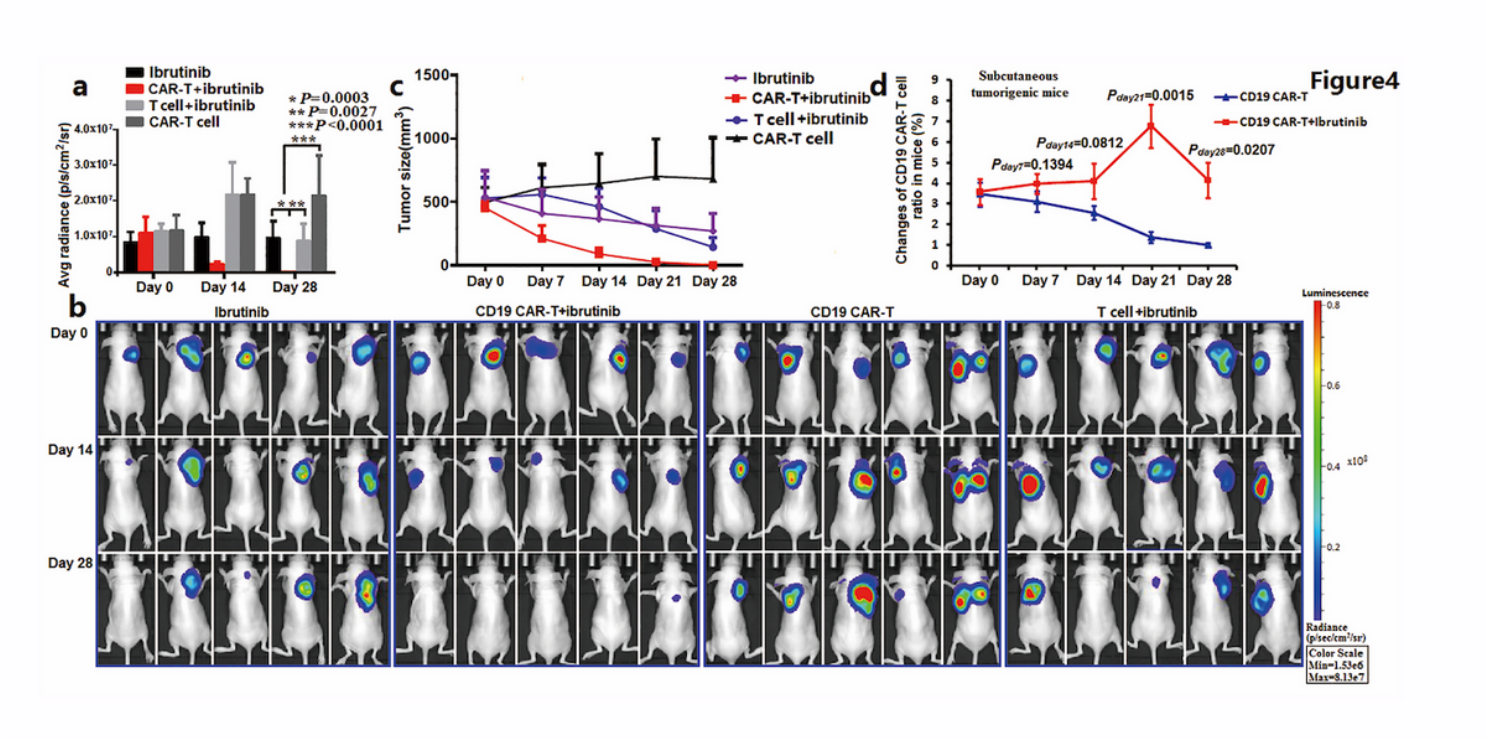

Figure 8

The combined effect of ibrutinib and CD19 CAR-T cells in subcutaneous tumorigenic model. a, c. The reduction in tumor size was greater in the ibrutinib combined with CD19 CAR-T cell polytherapy group than those in the other three groups. b. The extinction of luciferase expression was greater in the ibrutinib combined with CD19 CAR-T cell polytherapy group than that of the other three groups. d. The proportion of CD19 CAR-T cells was higher in the ibrutinib combined with CD19 CAR-T cell group than that of the CD19 CAR-T cell group on day 21 and day 28.

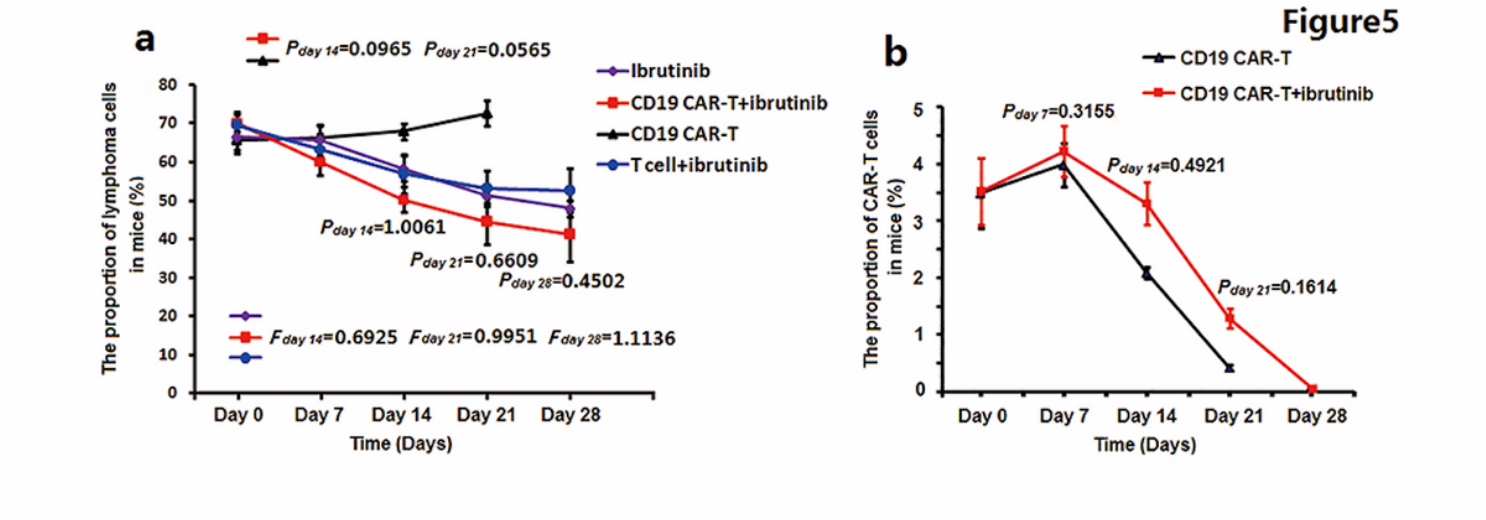

Figure 10

The combined effect of ibrutinib and CD19 CAR-T cells in tail vein tumorigenic model. a. There was no different of the proportion of lymphoma cells in the ibrutinib group, the ibrutinib combined with CD19 CAR-T cell group, and the ibrutinib combined with T cell group. b. There was no different of the proportion of CD19 CAR-T cells in the ibrutinib combined with CD19 CAR-T cell group and the CD19 CAR-T cell group on day 7, day 14, day 21 and day 28.

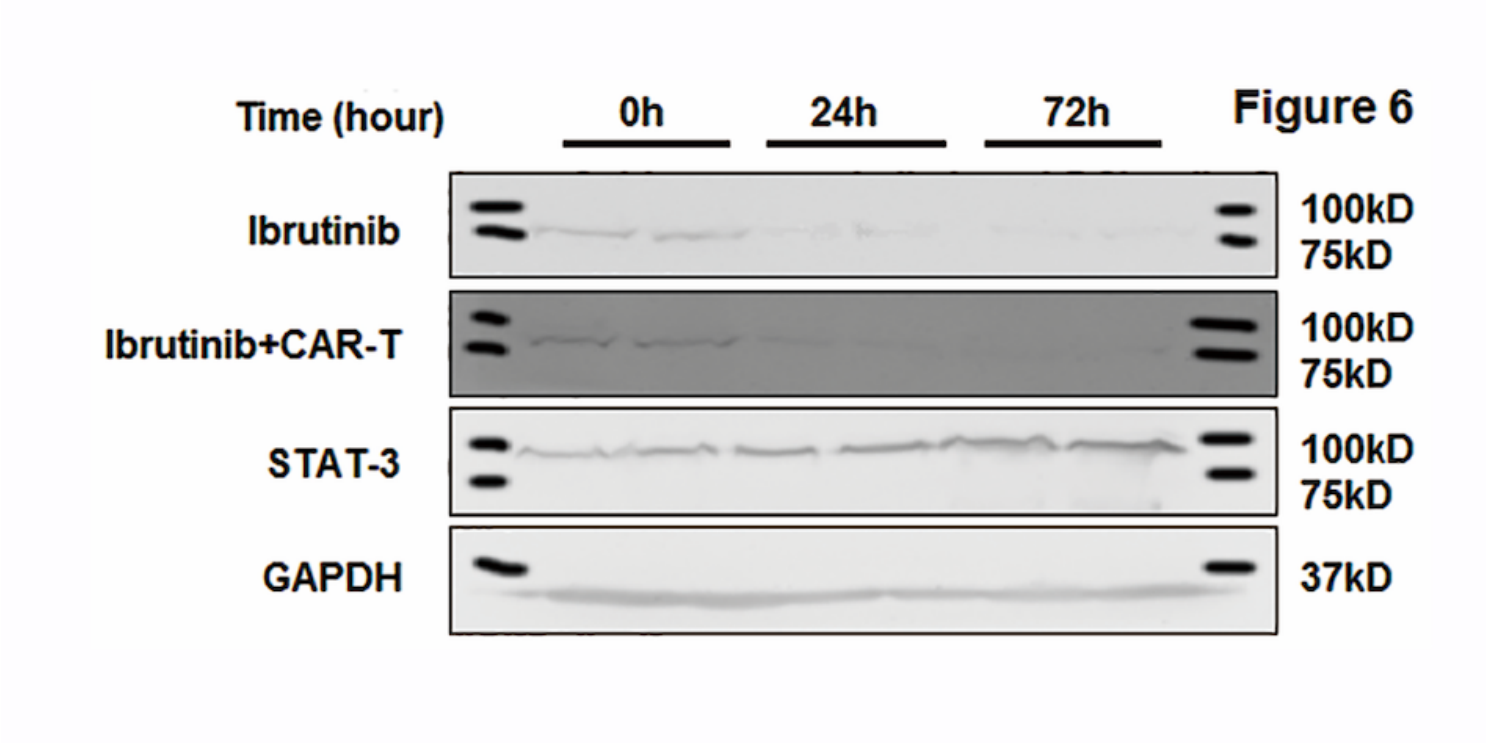

Figure 11

The expression of STAT-3 signaling pathway. There was no difference between the expression of STAT-3 in tumor cells in groups of ibrutinib with or without CD19 CAR-T cells.